Electron-Beam-Breakup Transit-Time Oscillator

Thomas J. T. Kwan
Applied Theoretical Physics Division, Los Alamos National Laboratory, Los Alamos, New Mexico 87545

Michael A. Mostrom and Brendan B. Godfrey[a]
Mission Research Corporation, Albuquerque, New Mexico 87106
(Received 4 February 1991)

The electron-beam-breakup transit-time oscillator has been investigated via theoretical analysis and computer simulation as a high-power microwave generator. Coupling the beam-breakup instability with the transit-time effect of the electron beam in the cavity, rapid energy exchange between the electrons and cavity modes can occur. Furthermore, the transit-time resonance naturally leads to narrow-band output. Driven by a high-current electron beam, the beam-breakup transit-time oscillator can be a compact source for high-power (>1 GW) operation. Good agreements have been obtained between linear theory and simulation.

PACS numbers: 85.10.Jz, 52.35.Hr, 52.65.+z

Many conventional high-power microwave sources[1] rely on the axial bunching of an electron beam to excite electromagnetic modes in various structures. Such bunching becomes increasingly difficult to produce as the beam energy γ increases; this causes the growth rate to decrease as $1/\gamma^3$ if it scales with the longitudinal beam plasma frequency. With space-charge-limited currents decreasing with lower voltages, high efficiency is difficult to achieve simultaneously with high power (>1 GW). The klystrode[2] offers a reasonably compact source which is capable of delivering microwave power at MW levels with high efficiencies, and the more complex relativistic klystron[3] can produce microwaves at a few 100 MW in the multigigahertz range. However, the klystrode efficiency decreases rapidly when the frequency goes beyond the gigahertz range. This decrease in efficiency in the high-frequency range puts a rather severe limitation on its application to high-average-current accelerators.

This problem is also true for the usual transit-time oscillators (TTO),[4] such as the monotron,[5,6] where a continuous electron beam passing axially through a simple pillbox cavity generates microwaves if the cavity dimensions are chosen correctly. Electrons traversing the cavity either gain or lose energy, depending on their transit time across the cavity and on the phase of the microwave fields when they enter. Those electrons that lose energy remain in the cavity longer than those that gain energy. Therefore, this creates the possibility of net energy transfer to the fields. However, the required axial bunching of the beam again results in unfavorable scaling with γ. Also the large value of the interaction Q implies that little power can be extracted from the cavity.

The beam-breakup transit-time oscillator (BTO) does not depend on axial bunching to facilitate energy exchange with the nonaxisymmetric electromagnetic modes. Essentially, in this device the electron beam is deflected sideways by the finite transverse magnetic field of a cavity mode such as TM_{110} or TE_{112}, and then the electron beam exchanges energy with the mode in proportion to $\mathbf{J}_\perp \cdot \mathbf{E}_\perp$ and to $J_z \nabla_\perp E_z \cdot \mathbf{X}_\perp$. Here $\mathbf{X}_\perp$ is the transverse displacement of the electron beam. The cavity mode grows or damps depending only on the transit time, $T = d/v$, of the electron beam with axial velocity v traveling across the cavity of length d. Because the growth depends only on transverse deflections of the beam as the beam energy increases, the growth rate decreases only as $1/\gamma$ and the efficiency remains nearly constant.

A standard small-signal gain analysis has been performed to obtain the growth rate of the TM_{110} mode in a pillbox cavity due to a continuous, axially injected, relativistic electron beam. The steps are as follows. First, the small-amplitude transverse deflections of the particles from their otherwise straight-line paths, caused by the electromagnetic mode, are computed. No applied axial magnetic field is present here. Equilibrium beam self-fields are ignored also. Second, energy gain by the fields is determined from $-\mathbf{J} \cdot \mathbf{E}$, where $\mathbf{J}$ is the perturbed beam current. The resulting expression is, of course, quadratic in the field amplitude. Third, if the electromagnetic mode has axial dependence, the energy-gain expression needs to be averaged over beam-injection phase angles. Fourth, the total field energy in the cavity is evaluated. Finally, the microwave growth rate is then obtained as one-half the ratio of the averaged rate of microwave energy gain to the stored microwave energy in the cavity.

We can express the vector potential of the TM_{110} cavity mode near the axis as

$$A_z = A_0[x\cos(\omega t - \phi) \pm y\sin(\omega t - \phi)] ,$$

where ω is the mode frequency. A_0 and ϕ are the field amplitude and injection phase angle. The field com-

ponents are given by

$$E_z = \omega A_0 [x \sin(\omega t - \phi) \mp y \cos(\omega t - \phi)] , \quad (1)$$

$$B_x = \pm A_0 \sin(\omega t - \phi), \quad B_y = -A_0 \cos(\omega t - \phi) . \quad (2)$$

The single-particle perturbed transverse position is described by

$$\gamma \ddot{x} = -vB_y = A_0 v \cos(\omega t - \phi) , \quad (3)$$

$$\gamma \ddot{y} = vB_x = \pm A_0 v \sin(\omega t - \phi) , \quad (4)$$

where the cavity transverse fields are evaluated at the unperturbed on-axis position of the particle; in our small-signal analysis we take v and γ to be its initial axial velocity and energy. The particle charge and mass, as well as the speed of light, are set equal to unity for notational simplicity here. Perturbed axial motion is unimportant because the particles are assumed relativistic. Solving Eqs. (3) and (4) gives

$$x = -\frac{A_0 v}{\gamma \omega^2} [\cos(\omega t - \phi) - \cos\phi] + \frac{A_0 v t}{\gamma \omega} \sin\phi , \quad (5)$$

$$y = \mp \frac{A_0 v}{\gamma \omega^2} [\sin(\omega t - \phi) + \sin\phi] \pm \frac{A_0 v t}{\gamma \omega} \cos\phi . \quad (6)$$

The change in particle energy in traversing the cavity is given by vE_z integrated along the perturbed path,

$$\Delta\gamma = \int_0^{d/v} v E_z \, dt = -\frac{A_0^2 v^2}{\omega^2 \gamma} \left[2\cos\frac{\omega d}{v} + \frac{\omega d}{v} \sin\frac{\omega d}{v} - 2 \right] . \quad (7)$$

The corresponding microwave power is obtained by multiplying $-\Delta\gamma$ from Eq. (7) by the beam density and integrating over the beam cross section. The result is

$$P = v\gamma \frac{A_0^2 v}{\omega^2} \left[\frac{\omega d}{v} \sin\frac{\omega d}{v} + 2 \left(\cos\frac{\omega d}{v} - 1 \right) \right] , \quad (8)$$

where v is the beam current, normalized to 17 kA. The microwave field energy in the cavity is defined in the usual manner, $U = \frac{1}{2} \int [E_z^2 + \mathbf{B}_\perp^2] dV$. The fields given in Eqs. (1) and (2) are valid only near the axis. Their general forms are in terms of the Bessel function J_1, and the field energy U is

$$U = d(J_1' R)^2 A_0^2 / 2 . \quad (9)$$

Here, J_1' is evaluated at $\chi_1 = k_\perp R$, the first zero of J_1, R is the cavity radius, and d is the axial length of the cavity. Finally, the microwave growth rate, or gain, is obtained by dividing P from Eq. (8) by $2U$ from Eq. (9). The resulting growth-rate expression is

$$\frac{\omega_i d}{v} = \frac{v}{\gamma} (J_1' \chi_1)^{-2} \left[2 \left(\cos\frac{\omega d}{v} - 1 \right) + \frac{\omega d}{v} \sin\frac{\omega d}{v} \right] . \quad (10)$$

Transit-time effects enter through the sine and cosine terms in Eq. (10). The growth rate ω_i is maximized for a transit time near $\omega d/v = (l + \frac{1}{2})\pi$, where l is an even nonzero integer. Note the maximum growth rate scales with the frequency ω of the cavity mode.

The growth rate in inverse nanoseconds from Eq. (10) is plotted as a function of the cavity thickness d (cm) in Figs. 1(a) and 1(b) for the cases of a cylindrical cavity with radius $R = 7.5$ cm, electron-beam energy $V = 2.55$ MV (0.51 MV), and electron-beam current $I = 5$ kA (0.8 kA). The velocity v is taken to be the initial injection velocity. Space-charge effects, which would tend to depress the actual velocity, have not yet been included. This is a good approximation for an electron beam with current much smaller than the space-charge-limited current. More complicated growth expressions for higher-order modes have been obtained by Godfrey *et al.*[7]

We have carried out detailed computer simulations to compare with the linear theory and more importantly to estimate the nonlinear saturation state which determines the efficiency of this microwave generator. Since the unstable modes in the BTO device are nonaxisymmetric, it is necessary to use a three-dimensional code to model the spatial variations of all physical quantities. The 3D particle-in-cell code IVORY, which represents azimuthal variations by Fourier modes, has been used successfully to model the physics of the BTO interaction in an unloaded cavity.

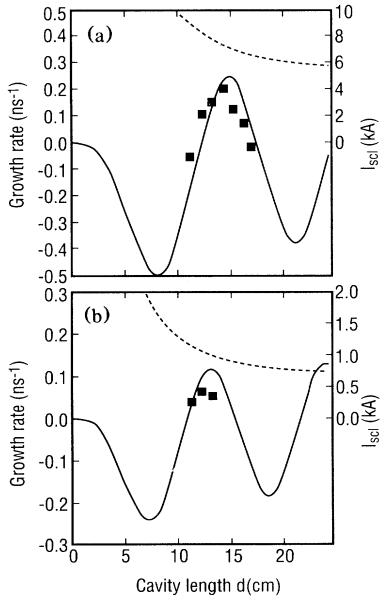

FIG. 1. BTO microwave-source growth rate vs cavity length. (a) Beam energy $V = 2.55$ MeV and current $I = 5$ kA, and (b) beam energy $V = 0.51$ MeV and current $I = 0.8$ kA. Solid lines are linear theory; points are IVORY simulations; dashed lines are space-charged-limited current in kiloamps. In the simulation results, the rms thermal angle was fixed at $P_\perp/P_z = 0.065$, and the cavity radius was 7.5 cm.

The simulations were performed in cylindrical geometry (z,r,θ). A solid relativistic electron beam is injected into a metallic cylindrical cavity which has already been primed with the TM_{110} cavity mode with the polarization chosen so that E_z varies as $\cos\theta$ with an amplitude of 50 kV/cm. With this polarization, the magnetic field at the cavity axis of symmetry lies along the x direction for the TM_{110} mode, and the beam is deflected in the y direction. The resistive loss at the cavity wall has only a very small effect in the interaction and is, therefore, ignored in the simulations. The purpose of priming the cavity is to facilitate the growth of the particular mode. The cavity has a radius of 7.5 cm and its length is varied among simulations to yield the functional dependence of the growth rate. The space-charge-limited current varies from 8.9 to 6.6 kA for $d=11-17$ cm. In one series of simulations, a solid electron beam of 5 kA and 2.55 MeV is injected into the cavity. The electron beam has a radius of 1.8 cm. Since no external magnetic field is imposed, the beam is given a Gaussian momentum distribution $(P_\perp/P_z=0.065)$ in the perpendicular direction (r,θ) to maintain radial equilibrium against self-magnetic pinching as it propagates across the cavity.

In Fig. 2, we show the time evolution of the transverse-magnetic cavity mode TM_{110} and its Fourier transform. The logarithmic field amplitude is also shown to confirm the linear growth rate. In this case, the length of the cavity is chosen to be 15 cm. The frequency and the growth rate of this mode are found to be 2.43 GHz and 0.12/ns, respectively. The magnitude of the growth rate can easily provide significant amplification of the cavity mode for any electron beam with pulse duration greater than 50 ns. Further increase in the growth rate can be obtained by choosing an optimal length of the cavity and/or by using a smaller cavity with higher TM_{110} frequency. A growth rate of 0.2/ns has been confirmed in our simulation with a cavity length of 14.0 cm.

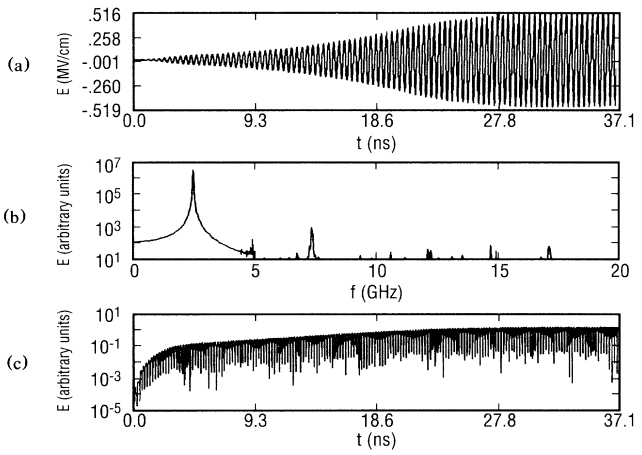

FIG. 2. For properly chosen beam transit time across the cavity, the beam-breakup instability can cause rapid growth of the transverse-magnetic cavity mode (TM_{110}). (a) Axial electric field E_z vs time, (b) E_z vs frequency, and (c) $\log E_z(t)$ vs time. Cavity length is $d=15$ cm.

The electron-beam dynamical behavior can be visualized by examining the phase-space structure of the electron beam at various times during the simulation. Figure 3 shows a snapshot of the electron-beam real space [y (i.e., $r\sin\theta$) vs z] and phase space [$mc^2(\gamma-1)$ vs z]. At this time, the instability has already saturated. As the electron beam enters the cavity, it is acted upon by an oscillatory radial (y-directed) force resulting from the azimuthal (x-directed) magnetic field of the cavity mode and its axially streaming motion. Consequently, the electron beam oscillates with increasing radial motion in the y direction as it propagates across the cavity. Eventually, the radial excursion of the beam can be large enough for it to strike the cavity wall, causing the energy-exchange process to stop. The energy phase-space diagram shows that some electrons at this particular time have lost in excess of 50% of their energy when they strike the outer wall of the cavity. The energy loss is converted into electromagnetic-field energy resulting in the strong excitation of the TM_{110} cavity mode. The average kinetic-energy loss of the electron beam when it exits the cavity is about 35%.

The comparison of the linear growth rate of TM_{110} observed in the simulations with the theoretical prediction for different lengths of the cavity is shown in Figs. 1(a) and 1(b). The cavity radius is fixed at $R=7.5$ cm, and two cases for the electron beam are shown: (a) beam energy $V=2.55$ MeV and current $I=5$ kA, as discussed above; and (b) a lower-energy beam with $V=0.51$ MeV and current $I=0.8$ kA. In both cases, our simulation results show a slight shift in the cavity length for maximum growth. We believe this is caused by the electron-beam space charge on its transit time across the

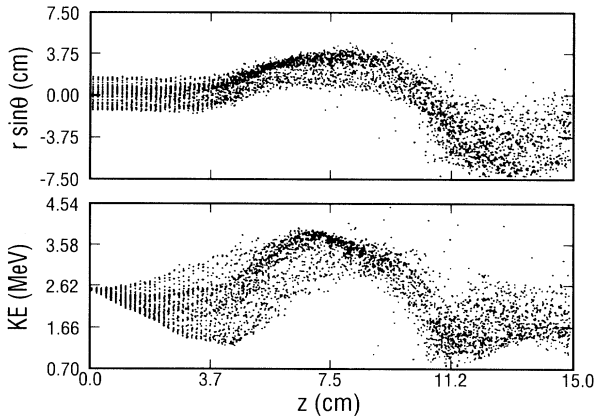

FIG. 3. Electron-beam behavior confirms the physical process of the beam-breakup transit-time oscillator.

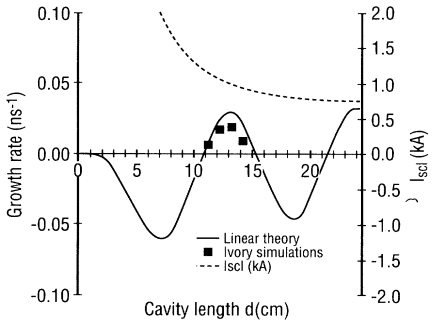

FIG. 4. The agreement between theory and simulation improves significantly when the electron-beam current is only a small fraction of the space-charge-limited current.

cavity. The slightly smaller growth rates obtained from the simulation may be due to the finite velocity spread of the electron beam (normalized emittance of 0.2 rad cm) whereas the theory uses a cold-beam approximation. However, the overall agreement is very good.

To confirm the effects of beam emittance on the growth rate, we increased the normalized beam emittance to 0.7 rad cm in our simulation, and the growth rate dropped as expected, but by only 40%. This points out a further advantage of this concept which has a rather mild dependence on the electron-beam quality.

We have also studied by computer simulation the effects of electron-beam space charge on the instability. In Fig. 1(b), the growth rate of the TM_{110} mode is shown for different cavity lengths for the electron beam with energy of 0.51 MeV and current of 0.8 kA. Since the space-charge-limited current for the electron beam is about 1 kA, the substantial radial variation of the electron-beam velocity is expected to affect the growth rate. The comparison between the linear theory which neglects the space-charge effect and the simulation confirms the deviation. The simulation results of the electron beam with a lowered beam current of 0.2 kA are shown in Fig. 4. Here the space-charge effect is much less important and the agreement is significantly improved.

Our linear theory and computer simulation show that the BTO appears to be a promising high-power microwave source. A large linear growth rate ($> 10\%$/cycle) has been confirmed in our theory and computer simulations. This results in the possibility of high-power extraction from the cavity without quenching the microwave generation. The efficiency of energy conversion from the electron beam to microwave radiation has been shown to be significant. Furthermore, it is not sensitive to the microwave frequency and has only a very mild dependence on the electron-beam energy. These characteristics can greatly facilitate its applications, ranging from high-gradient accelerators to plasma heating in fusion experiments.

We would like to thank T. Genoni, M. Campbell, and T. Hughes for many useful discussions. The work by T. Kwan was supported by the U.S. DOE.

[a]Present address: Phillips Laboratory, Albuquerque, NM 87111.

[1]*High-Power Microwave Sources,* edited by Victor L. Granatstein and Igor Alex-Alexeff (Artech House, Boston, 1987).

[2]D. H. Preist and M. B. Shrader, Proc. IEEE **70**, 1318 (1982).

[3]M. A. Allen *et al.*, Phys. Rev. Lett. **63**, 2472 (1989).

[4]D. Marcuse, *Principles of Quantum Electronics* (Academic, New York, 1980), pp. 125–144.

[5]F. B. Llewellyn and A. E. Bowen, Bell Syst. Tech. J. **18**, 280 (1939).

[6]J. Marcum, J. Appl. Phys. **17**, 4 (1946).

[7]B. B. Godfrey, D. J. Sullivan, M. J. Arman, T. C. Genoni, and J. E. Walsh, Proc. SPIE Int. Soc. Opt. Eng. **1061**, 84 (1989).